


4-Deoxy- ϵ -Pyrromycinone: A Promising Drug/Lead Compound to Treat Tumors

Jiping Zhang ^{*}, Xianan Sang^{*}, Yichao Yuan, Jiawei Shen, Yuanyuan Fang, Minjing Qin, Hangsheng Zheng, Zhihong Zhu

College of Pharmaceutical Science, Zhejiang Chinese Medical University, Hangzhou, 311402, People's Republic of China

^{*}These authors contributed equally to this work

Correspondence: Hangsheng Zheng; Zhihong Zhu, College of Pharmaceutical Science, Zhejiang Chinese Medical University, Hangzhou, People's Republic of China, Email hs-zheng@163.com; zzhjanny@163.com

Background: Anthraquinone drugs are widely used in the treatment of tumors. However, multidrug resistance and severe cardiac toxicity limit its use, which have led to the discovery of new analogues. In this paper, 4-Deoxy- ϵ -pyrromycinone (4-Deo), belonging to anthraquinone compounds, was first been studied with the anti-tumor effects and the safety in vitro and in vivo as a new anti-tumor drug or lead compound.

Methods: The quantitative analysis of 4-Deo was established by UV methodology. The anti-cancer effect of 4-Deo in vitro was evaluated by cytotoxicity experiments of H22, HepG2 and Caco2, and the anti-cancer mechanism was explored by cell apoptosis and cycle. The tumor-bearing mouse model was established by subcutaneous inoculation of H22 cells to evaluate the anti-tumor effect of 4-Deo in vivo. The safety of 4-Deo was verified by the in vitro safety experiments of healthy cells and the in vivo safety experiments of H22 tumor-bearing mice. Tumor tissue sections were labeled with CRT, HMGB1, IL-6 and CD115 to explore the preliminary anti-cancer mechanism by immunohistochemistry.

Results: In vitro experiments demonstrated that 4-Deo could inhibit the growth of H22 by inducing cell necrosis and blocking cells in S phase, and 4-Deo has less damage to healthy cells. In vivo experiments showed that 4-Deo increased the positive area of CRT and HMGB1, which may inhibit tumor growth by triggering immunogenic cell death (ICD). In addition, 4-Deo reduced the positive area of CSF1R, and the anti-tumor effect may be achieved by blocking the transformation of tumor-associated macrophages (TAMs) to M2 phenotype.

Conclusion: In summary, this paper demonstrated the promise of 4-Deo for cancer treatment in vitro and in vivo. This paper lays the foundation for the study of 4-Deo, which is beneficial for the further development anti-tumor drugs based on the lead compound of 4-Deo.

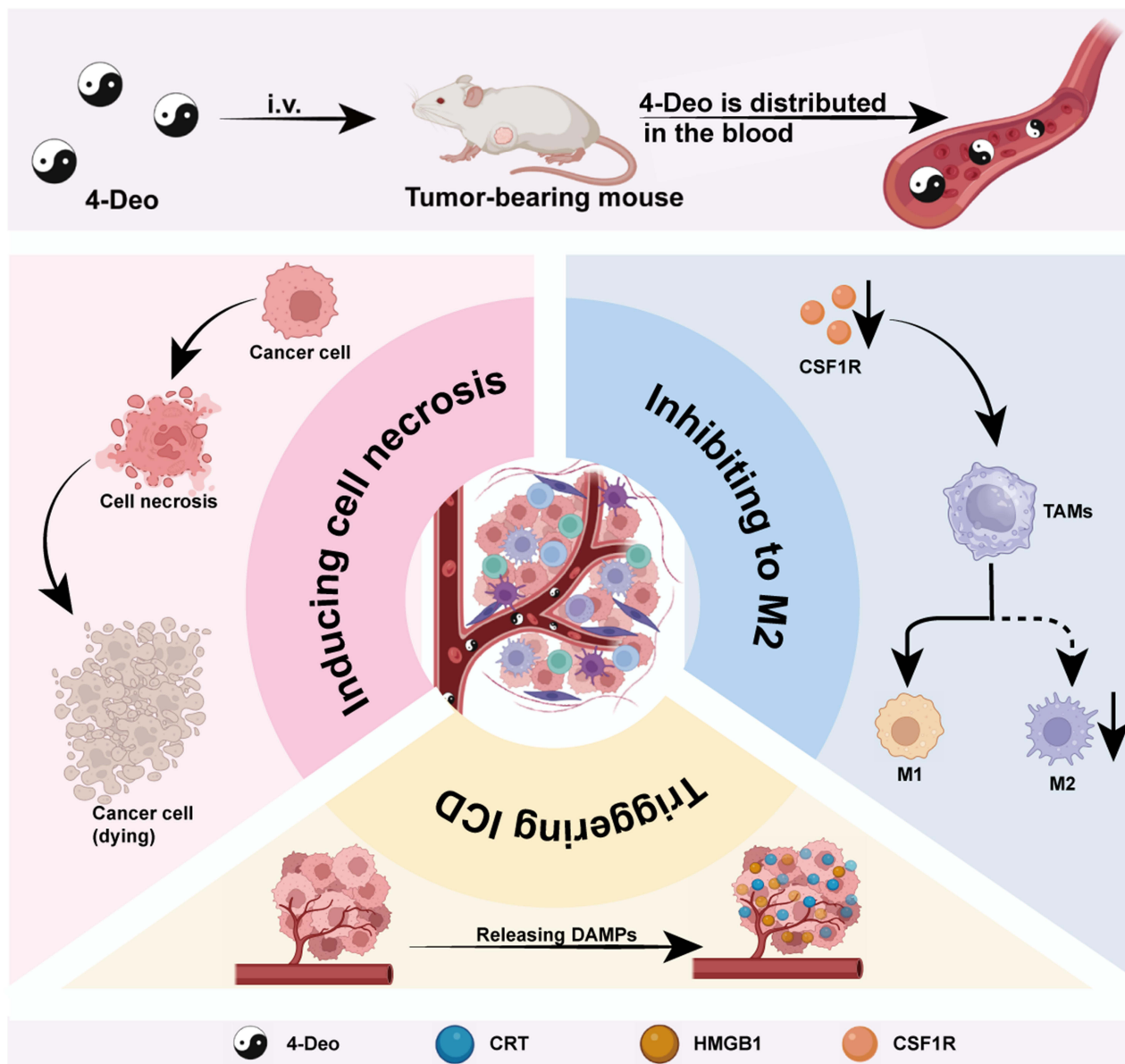
Keywords: 4-deoxy- ϵ -pyrromycinone, lead compound, drug safety, drug efficacy, anti-tumor drug

Introduction

According to the International Agency for Research on Cancer, there were close to 20 million new cases of cancer alongside 9.7 million cancer deaths in 2022.¹ These data show that the threat of cancer to human life and health is increasing, so the search for new drugs or new therapeutic targets is essential for the treatment of cancer. Even though macromolecular drugs have been attracting more and more attention, especially since the occurrence of novel coronavirus pneumonia,^{2,3} the development of small molecular drugs is still one of the focuses of new drug development. Compared with macromolecular drugs, small molecule drugs can avoid the local or systemic adverse reactions caused by excipients and the sensitivity of proteins to pH, have higher stability, and in particular, reduce the cost of drug development.⁴ What's more, small molecule drugs can be obtained in more diverse ways.

When our team subjected *Streptomyces* sp. BG-11 to large-scale fermentation, which was isolated from rhizosphere soils of the plant *Atractylodes macrocephala* Koidz from Zhejiang Province, China, we found that the fermentation

Graphical Abstract



products had antitumor ability. After several isolation screens and comparison with the literature, we found it is the 4-Deoxy- ϵ -pyrromycinone (4-Deo).^{5,6} 4-Deo belongs to anthraquinone compounds. As we all know, anthraquinone drugs, including daunorubicin, doxorubicin, epirubicin, pirarubicin, aclamycin, etc. are widely used in the treatment of hematological malignancies and solid tumors.⁷⁻⁹ However, regardless of its therapeutic effects, multidrug resistance and severe cardiac toxicity are important limitations of anthracycline drug therapy, which have led to the discovery of new analogues.¹⁰⁻¹² The structure of 4-Deo is similar to that of commonly used clinical compounds, both of which have a four membered ring mother nucleus. However, 4-Deo has an additional carboxyl group in its structure, making it a lead compound for anti-tumor drugs. More importantly, through literature review, we found that current research only determined the structure of the compound⁵ and only Aiai's paper has proved its anticancer activity in vitro.¹³ Based on the previous research foundation of our team and the good anti-tumor effects of anthraquinone compounds, we

decided to systematically study the anti-tumor effects and the safety of 4-Deo, as a new anti-tumor drug or lead compound, in vitro and in vivo for the first time.

Materials and Methods

Materials

4-Deoxy- ϵ -pyrromycinone (4-Deo) was isolated and confirmed by the laboratory (see Supporting Information Experimental section 1.1 and 1.2). Doxorubicin hydrochloride (DOX) (cat. no. S17092-100mg) was purchased from Shanghai yuanye Bio-Technology Co., Ltd. 3-(4,5-dimethylthiazol-2)-2,5-diphenyltetrazolium bromide salt (MTT) (cat. no. ST316), Erythrocyte lysate (cat. no. C3702) and trypsin-EDTA solution (0.25% trypsin) (cat. no. C0201-500mL) were purchased from Beyotime Biotechnology Co., Ltd. (Shanghai, China). Cell cycle and apoptosis analysis kit (cat. no. BL114A) and cell counting kit-8 (CCK-8) (cat. no. BS350B) were purchased from Beijing Labgic Technology Co., Ltd. (Beijing, China). Annexin V-FITC apoptosis detection kit (cat. no. C1062M) and CD115/CSF-1R Rabbit Monoclonal Antibody (cat. no. AG1701) were purchased from Beyotime Biotechnology Co., Ltd. (Shanghai, China). Anti-Calreticulin antibody (cat. no. AB92516) and Anti-HMGB1 antibody (cat. no. AB79823) were purchased from Abcam (Cambridge, UK). Anti-CD86 Rabbit mAb (cat. no. GB13585) and Anti-IL-6 Rabbit pAb (cat. no. GB11117) were purchased from Servicebio Biotechnology Co., Ltd. (Wuhan, China). All chemicals are of analytical grade.

Cell Culture

L929 cells were purchased from National Collection of Authenticated Cell Cultures (Shanghai, China) and cultured in MEM medium supplemented with 10% (v/v) HI horse serum and 1% (v/v) non-essential amino acids. Mouse liver cancer cells (H22), human hepatocellular carcinoma cells (HepG2), human colorectal adenocarcinoma cells (Caco2), mouse monocyte macrophage leukemia cells (RAW264.7), immortalized rat renal proximal tubule cells (NRK-52E), human bronchial epithelial cells (BEAS-2B), rat liver epithelial cells (WB-F344) and hepatic stellate cells (HSC) were purchased from National Collection of Authenticated Cell Cultures (Shanghai, China) and cultured in DMEM medium supplemented with 10% (v/v) FBS and 1% (v/v) penicillin-streptomycin. All cells were cultured in 5% CO₂ at 37°C. HepG2 cells have been authenticated by STR profile before the experiment.

Animals

Male Kunming (KM) mice (weight 25 ± 10 g) were provided by the Laboratory Animal Research Center, Zhejiang Chinese Medical University (Hangzhou, China). The protocol was approved by the Animal Experimental Ethics Committee of Zhejiang Chinese Medical University. The experimental animal welfare ethics is implemented according to the national standard of the People's Republic of China (GB/T 42011–2022). The ethical number is IACUC-20190527-02.

Ultraviolet Methodology Study

Since 4-Deo did not peak in conventional HPLC, it was analyzed by UV-visible spectrophotometer.

Determination of Maximum Absorption Wavelength

The maximum absorption wavelength (λ_{\max}) of the 4-Deo was obtained by scanning 40 $\mu\text{g}/\text{mL}$ 4-Deo in the range of 230–999 nm using Synergy H1 Enzyme Labeler (Burton, USA) at room temperature.

Drawing of 4-Deo Standard Curve

The 4-Deo of 5, 10, 15, 20, 24 $\mu\text{g}/\text{mL}$ were used to draw the standard curve by measuring the absorbance at λ_{\max} using a UV-visible spectrophotometer (UV2600A, Unico Instrument Co., Shanghai, China).

Durability

The 4-Deo with concentrations of 10, 16, 20 $\mu\text{g/mL}$ were used the same method to prepare, and the absorbance was measured at λ_{max} at 0, 1, 2, 4, 8, 12, 24, 48, 72 h, respectively.

Accuracy and Precision

The accuracy and precision of the detection method were investigated with 4-Deo at concentrations of 10, 15 and 20 $\mu\text{g/mL}$.

In vitro Effectiveness Assay of 4-Deo

In vitro, the effect of 4-Deo on cancer cells was investigated through cytotoxicity, cell cycle, and apoptosis experiments. DOX was used as a positive control for all experiments.

Cell Viability Assay

CCK8 assay on H22 cells: In 96-well plates, H22 cells were placed at 1×10^4 cells per well in 100 μL DMEM medium, and then treated with 4-Deo of 0.625, 1.25, 2.5, 5, 10 and 20 $\mu\text{g/mL}$ at 37°C and 5% CO_2 for 24 h. CCK8 (cat. no. BS350B) was added to each well and incubated for 4 h, finally, the absorbance was detected at 450 nm by using Synergy H1 Enzyme Labeler (Burton, USA).

MTT assay on HepG2 and Caco2 cells: In 96-well plates, HepG2 cells were placed at 5×10^3 cells per well in 100 μL DMEM medium, and then treated with 4-Deo of 0.3125, 0.625, 1.25, 2.5 and 5 $\mu\text{g/mL}$ at 37°C and 5% CO_2 for 24 h. MTT was added to each well for co-incubation. After 4 h, the supernatant was removed, and 100 μL DMSO was added to dissolve the crystals. The absorbance was detected at 570 nm by using Synergy H1 Enzyme Labeler (Burton, USA). Caco2 cells were treated with 4-Deo of 1.25, 2.5, 5, 10 and 20 $\mu\text{g/mL}$.

Cell Apoptosis

H22 cells were placed in 2.5 mL DMEM medium with 5×10^6 cells per well, and then respectively incubated with 0.25 mL, 2.2 $\mu\text{g/mL}$ 4-Deo for 24 h at 37°C and 5% CO_2 . Subsequently, Annexin V-FITC apoptosis detection kit (cat. no. C1062M) was used for treatment. The treated H22 cells were centrifuged at 1000 g for 5 min, and the precipitate obtained after washing with PBS was resuspended with Annexin V-FITC binding buffer. Annexin V-FITC and PI staining solution were added in order and incubated in dark at 25°C for 20 min and detected by CytoFlex flow cytometry.^{14,15}

Cell Cycle Assay

H22 cells were placed in 2.5 mL DMEM medium with 5×10^6 cells per well, and then respectively incubated with 0.25 mL, 2.2 $\mu\text{g/mL}$ 4-Deo for 24 h at 37°C and 5% CO_2 . Cell cycle and apoptosis analysis kit (cat. no. BL114A) were then used for processing. The treated H22 cells were centrifuged at 1000 g for 5 min, and the precipitate obtained after washing with PBS was resuspended with 70% ethanol. After overnight fixation, H22 cells were centrifuged at 1000 g for 5 min, and the precipitate was washed with PBS, re-suspended with PI staining solution and incubated at 37°C for 30 min in the dark, and detected by CytoFlex flow cytometry.

In vitro Safety Assay of 4-Deo

NRK-52E, BEAS-2B, WB-F344, HSC and L929 cells were used to evaluate the safety of 4-Deo. All cells were incubated overnight in 96-well plates with 1×10^4 cells per well and then incubated with 4-Deo of 2.5, 5, 10, 20 and 40 $\mu\text{g/mL}$ at 37°C and 5% CO_2 for 24 h. Subsequent operations were treated by MTT assay and the absorbance was detected at 570 nm by using Synergy H1 Enzyme Labeler.¹⁶

In vivo Tumor Growth Assay

H22 cells were inoculated subcutaneously into the right forelimb of mice at 3×10^6 / mouse. When the tumor volume grew to $\sim 150 \text{ mm}^3$, the mice were randomly divided into three groups with 5 mice in each group: control group, DOX group and 4-Deo group. Every three days, the body weight and tumor volume of tumor-bearing mice were recorded, and then

0.1 mL DOX or 4-Deo (4 mg/kg) was injected into the tail vein of corresponding group, and the control group was injected with physiological saline solution. According to animal ethics, the endpoint of the experiment was determined when the tumor diameter exceeded 15 mm or when the tumor site became ulcerated or infected. The mice were euthanized, and their tumors, hearts, livers, spleens, lungs, and kidneys were removed and stored in 4% paraformaldehyde. The therapeutic effect of 4-Deo on liver cancer was investigated by comparing the size of tumor volume. The tumor volume was calculated according to the width² × length / 2.

In vivo Safety Assay of 4-Deo

At the end of the experiment, the mice were euthanized and their hearts, livers, spleens, lungs, and kidneys were removed, fixed in 4% paraformaldehyde, and embedded in paraffin to make tissue sections. First, the sections were placed in hematoxylin staining solution to stain the nucleus, then put it into the eosin staining solution to stain the cytoplasm, and the effects of 4-Deo on the main organs were observed by HE staining.

Mechanism Exploration

Immunohistochemical analysis of tumor sections was performed using antibodies for CD86 (cat. no. GB13585), CRT (cat. no. AB92516), HMGB1 (cat. no. AB79823), IL-6 (cat. no. GB11117) and CD115/CSF-1R (cat. no. AG1701). At the end of the experiment, the mice were euthanized, and their tumors were fixed with 4% paraformaldehyde and embedded in paraffin. Tissue sections were dewaxed and rehydrated, and then sections were incubated with the primary antibody in a humid environment at 4°C overnight and rinsed with PBS three times. Then the secondary antibody of the same genus as the primary antibody was added dropwise and incubated at room temperature in dark for 50 min. After immunostaining, the sections were incubated with 1 µg/mL DAPI in the dark for 5 min to label the nucleus. ImageJ software was used to analyze the positive rate area.

Statistical Analysis

The experimental data were expressed as mean ± SD. We used GraphPad Prism 8 software to perform independent *t*-test and one-way analysis of variance (ANOVA) on the results. *P* < 0.05 was considered statistically significant (ns: *p* > 0.05, **p* < 0.05, ***p* < 0.01, ****p* < 0.001).

Results and Discussion

Ultraviolet Methodology Study

The maximum absorption wavelength (λ_{\max}) of the 4-Deo was determined and the standard curve was established to facilitate the quantification of 4-Deo concentration in subsequent experiments. The λ_{\max} of the 4-Deo was determined to be 492 nm by wavelength scanning (Figure 1A), and the OD value of anhydrous ethanol was lower than 0.05 under this condition (Figure 1B), which met the requirements of the Chinese Pharmacopoeia 2020 Edition (Volume IV 0401) for solvents in UV-visible spectrophotometry. The standard curve of the 4-Deo was $Y=0.03169X+0.009179$ ($R^2=0.9996$), which has a good linear relationship in the range of 5–24 µg/mL (Figure 1C). Precision, accuracy and durability are in accordance with the requirements of the Chinese Pharmacopoeia 2020 Edition (Volume IV 9101) ([Supplementary Table S1-S3](#)).

In vitro Efficacy and Safety Evaluation of 4-Deo

The quality characteristics of a drug include safety and efficacy. The problems caused by drug safety and efficacy are harmful to social harmony, so ensuring drug safety and efficacy are one of the most important problems at present. In this paper, the efficacy and safety of 4-Deo were investigated in vitro. The cytotoxicity, apoptosis and cell cycle assays were used to investigate the efficacy of 4-Deo. Both CCK8 assays and MTT assays showed that the cytotoxicity of 4-Deo on tumor cells was concentration-dependent. The 4-Deo could achieve the similar effect as DOX at high concentrations (Figure 2A-C). Cytotoxicity experiments showed that 4-Deo had an inhibitory effect on cancer cells in vitro, which was consistent with Aiai's paper.¹³

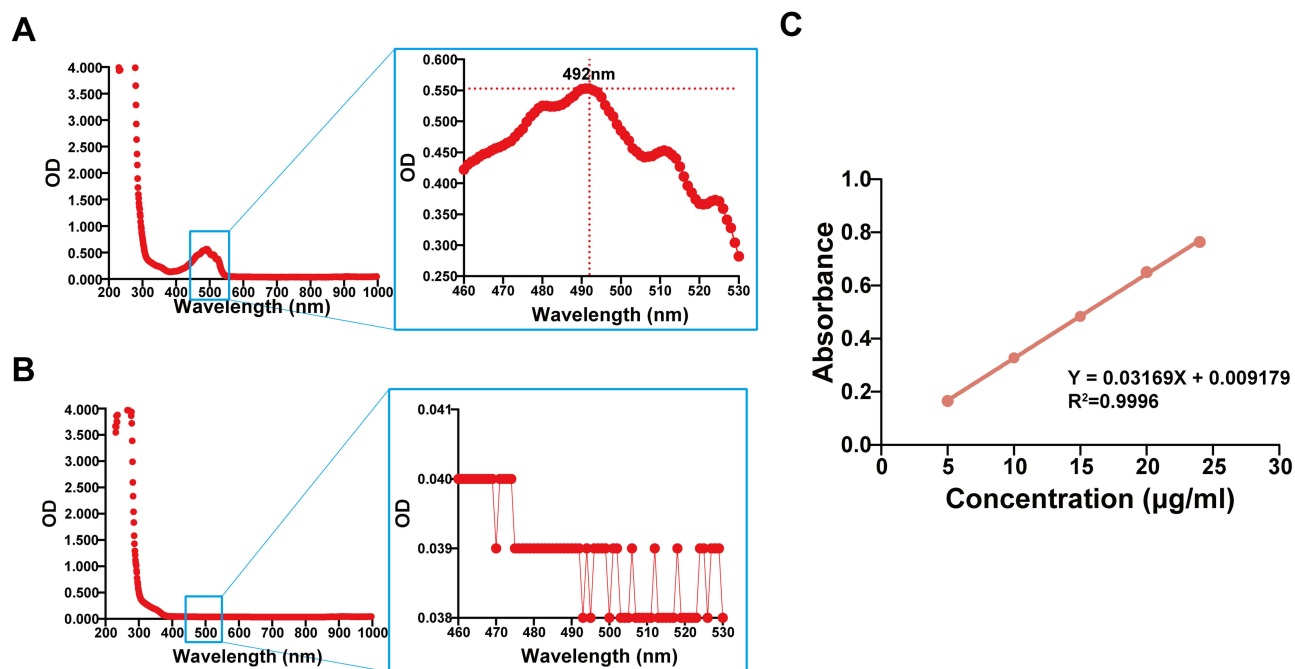


Figure 1 The maximum absorption wavelength and standard curve of 4-Deo. (A) The wavelength scanning of 4-Deo (40 µg/mL) in 230–999 nm. (B) The wavelength scanning of anhydrous ethanol in 230–999 nm. (C) The standard curve of 4-Deo in the range of 5–24 µg/mL.

In the apoptosis assay, it could be seen that under high concentration (5, 10, 20 µg/mL) (see Supporting Information Experimental section 1.3), both 4-Deo and DOX caused almost total apoptosis of H22 cells ([Supplementary Figure S1](#)). At the concentration of 0.2 µg/mL, the results of Annexin V-FITC/PI double staining showed that 4-Deo could induce more apoptosis than DOX, which may be caused by the regulation of apoptosis-related proteins, such as down-regulation of BCL-2 expression and up-regulation of BAX expression.^{14,17,18} DOX can inhibit cancer cell proliferation through reactive oxygen species production (ROS), apoptosis, senescence, autophagy, ferroptosis and pyroptosis induction, while 4-Deo inhibits cancer cell proliferation by different ways.¹⁹ It could be seen that 4-Deo induced almost 60.2% cells necrosis, while DOX only 1.13% ([Figure 2D](#)), which may be due to the fact that 4-Deo activated the receptor-interacting protein kinase and mixed lineage kinase-like pseudokinase related pathway (RIPK1-RIPK3-MLKL pathway).^{20,21} The results showed that 4-Deo mainly inhibited proliferation by inducing cell necrosis, which was different from DOX-induced apoptosis.^{18,19} However, some studies have shown that tumor cells have apoptosis resistance,^{22,23} apoptosis can even promote tumor progression by stimulating repair and regeneration in the tumor microenvironment,²⁴ so that drugs could not achieve the expected effect. And papers have shown that inducing necroptosis has advantages in overcoming apoptosis resistance, thereby improving anti-tumor efficiency.^{25–27} Therefore, 4-Deo may have an anti-tumor effect by inducing cell necrosis to overcome the apoptosis resistance of tumor cells. Cell cycle is an important evaluation index of anticancer drugs,²⁸ which was used to explore the effect of 4-Deo on the proliferation of H22 cells in this study. The cell cycle assay showed that both 4-Deo and DOX blocked H22 cells in the S phase ([Figure 2E](#)), which may be caused by up-regulating the expression of cell cycle regulatory proteins, as like P53 and P21.^{29,30} In summary, it was speculated that 4-Deo may play an anti-tumor role by inducing necrosis of H22 cells and blocking them in S phase, but the specific mechanism was not clear, which needed the further investigation.

The safety of 4-Deo and DOX were examined in the next step. It is well known that chemotherapy drugs can easily cause strong liver and kidney toxicity, which limits their clinical application.^{31,32} Therefore, BEAS-2B, WB-F344, HSC, NRK-52E and L929 cells were used to investigate the safety of 4-Deo. The results showed that all cells are consistent with the concentration dependence of DOX³³ and 4-Deo had more significant safety than DOX ([Figure 3](#)).

In conclusion, considering the efficacy and safety of 4-Deo in the treatment of liver cancer at the cellular level, its research prospects are surprising.

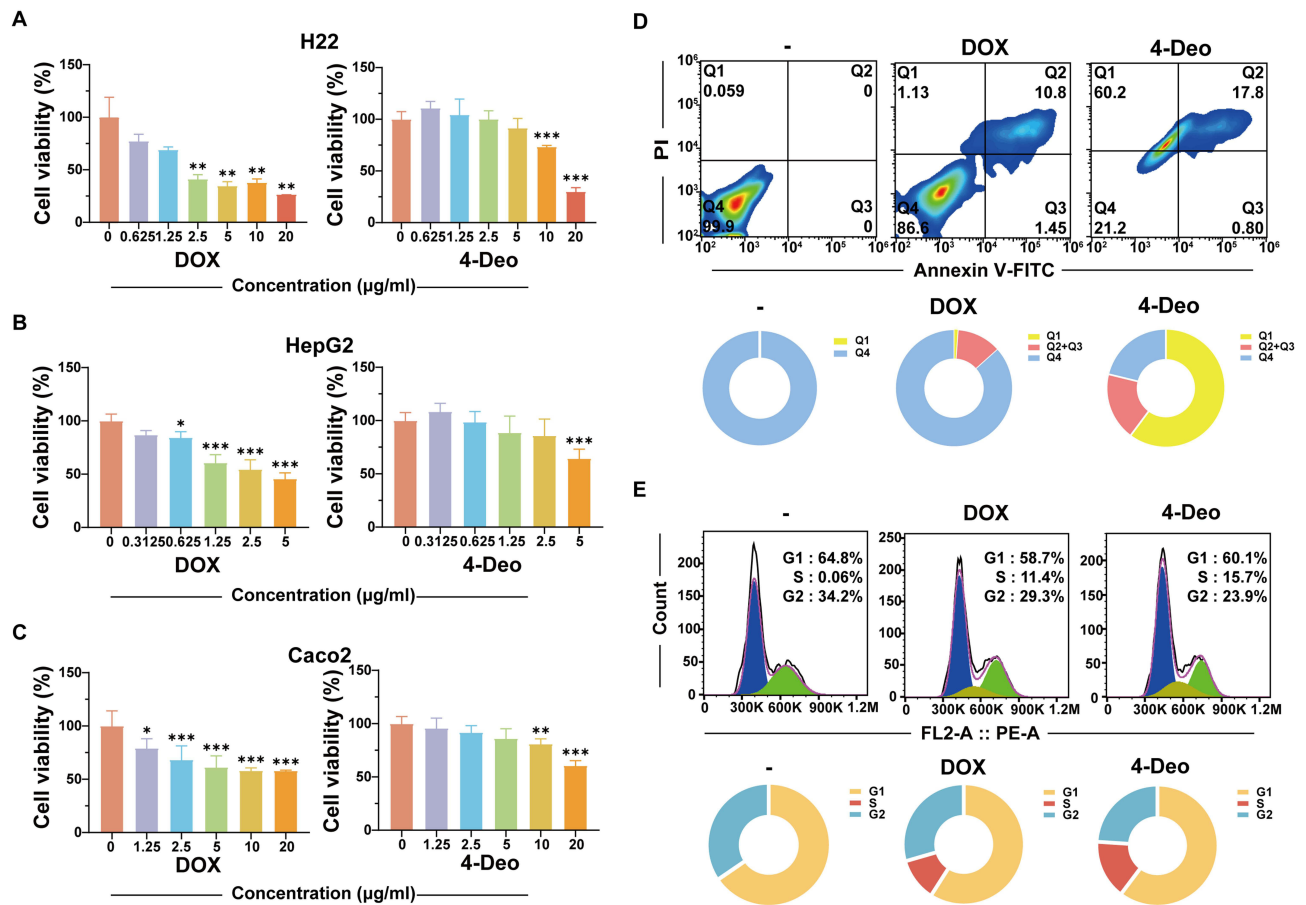


Figure 2 In vitro efficacy evaluation of 4-Deo. (A) The cytotoxicity of DOX or 4-Deo on H22 cells was determined by CCK8 assay. Data are presented as mean ± SD (n = 6). (B) The cytotoxicity of DOX or 4-Deo on HepG2 cells was determined by MTT assay. Data are presented as mean ± SD (n = 6). (C) The cytotoxicity of DOX or 4-Deo on Caco2 cells was determined by MTT assay. Data are presented as mean ± SD (n = 6). (D) H22 cells were treated with 0.2 μg/mL DOX or 4-Deo for 24 h and flow cytometry were used to detect cell apoptosis. (E) H22 cells were treated with 0.2 μg/mL DOX or 4-Deo for 24 h and flow cytometry were used to detect cell cycle. *p < 0.05, **p < 0.01, ***p < 0.001.

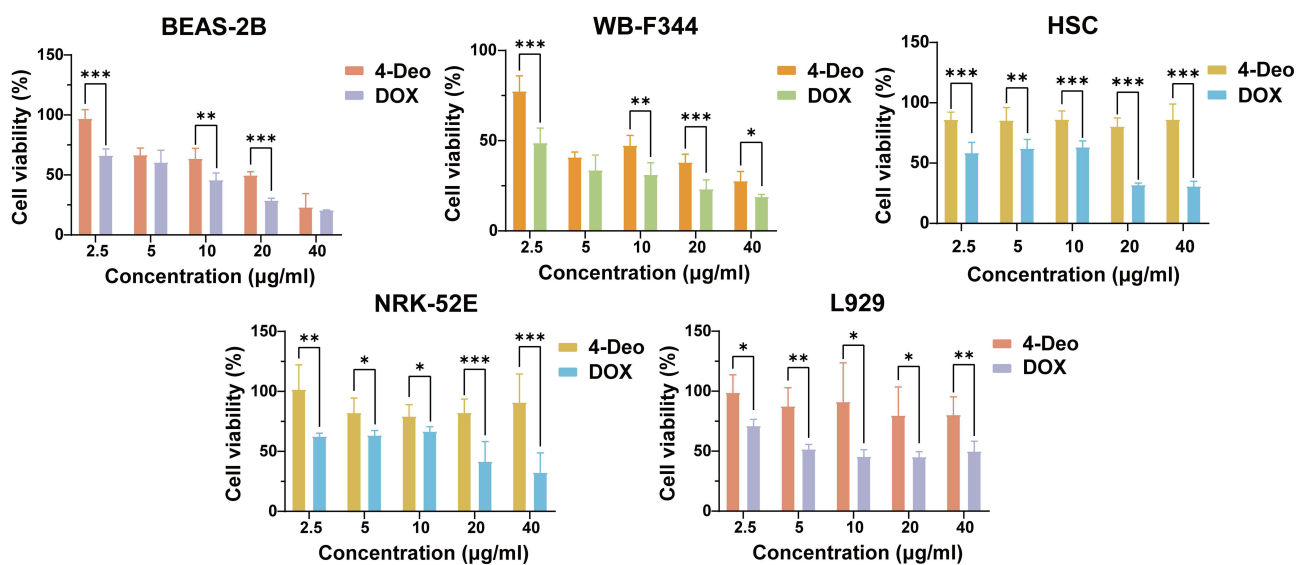


Figure 3 In vitro safety evaluation of 4-Deo. The cytotoxicity of DOX and 4-Deo on BEAS-2B, WB-F344, HSC, NRK-52E and L929 cells was determined by MTT assay. Data are presented as mean ± SD (n = 6). *p < 0.05, **p < 0.01, ***p < 0.001.

In vivo Tumor Growth Assay of 4-Deo

Cell apoptosis and cycle assays of 4-Deo demonstrated its inhibitory effect on tumor cells. In addition, the damaging effect of 4-Deo on healthy cells was significantly lower than that of DOX. Therefore, the tumor-bearing mouse assay was designed to further investigate the possibility of 4-Deo as a promising lead compound through in vivo assays. The tumor-bearing mice with tumor volume up to $\sim 150 \text{ mm}^3$ were randomly divided into three groups with 5 mice in each group. The tumor volume and body weight of the mice were recorded every three days, and physiological saline solution, DOX or 4-Deo were injected into the tail vein, respectively.

From Figure 4A, compared with the control group, both 4-Deo and DOX significantly played a role in inhibiting tumor growth, and both inhibition effects were comparable. As can be seen from the survival curves of the mice, at the end of the experiment, there was an 80% survival rate in the 4-Deo group, which was much higher than the 40% in the

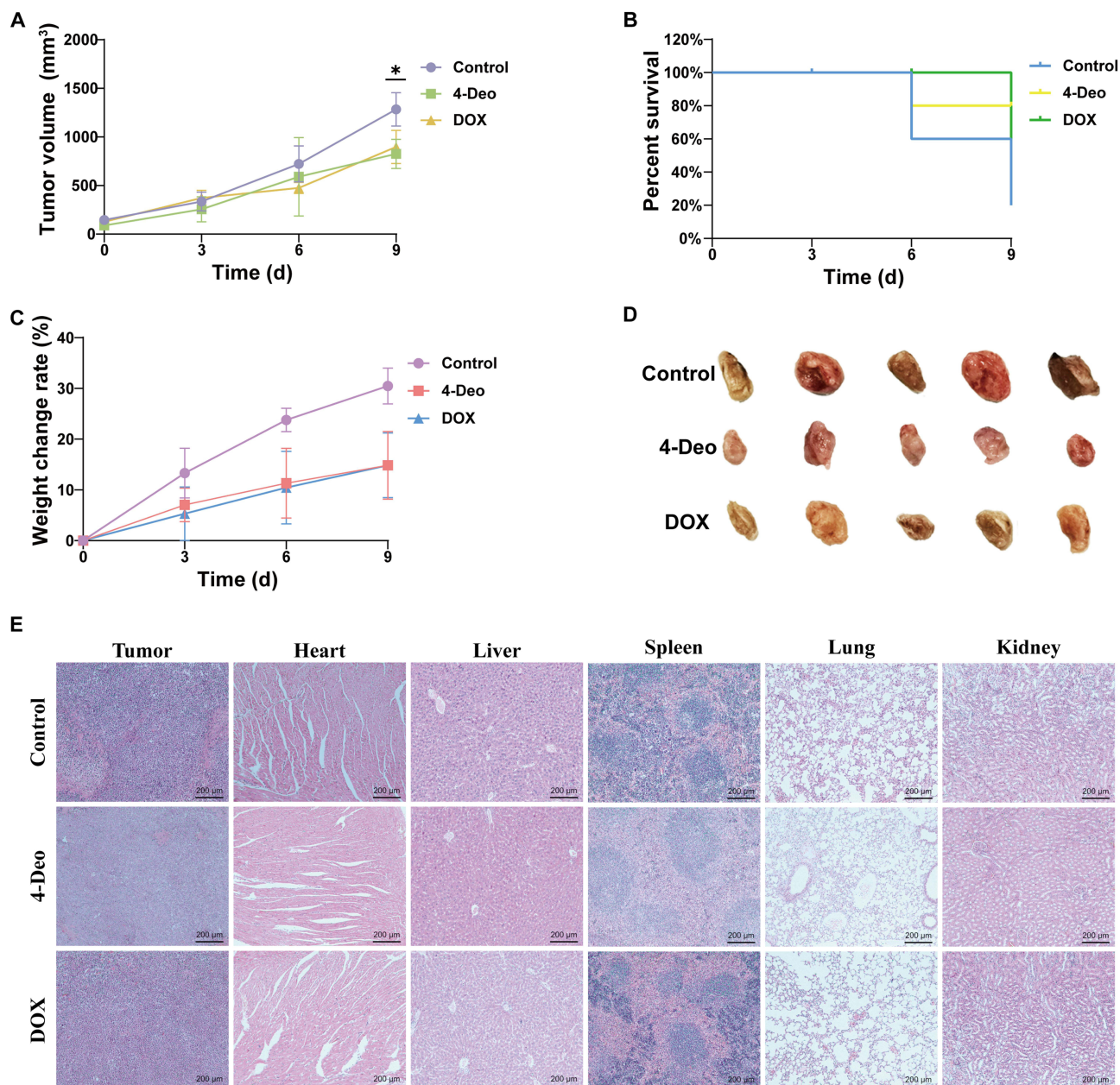


Figure 4 In vivo tumor growth assay of 4-Deo. (A) Tumor volume at different time points, data are presented as mean \pm SD ($n = 5$). (B) Survival curve of mice for different treatment groups. (C) Body weight change rate of different treatment groups during the assay schedule, data are presented as mean \pm SD ($n = 5$). (D) Image of solid tumor at end of life or experiment in mice. (E) Histological examination at the end of the experiment. * $p < 0.05$.

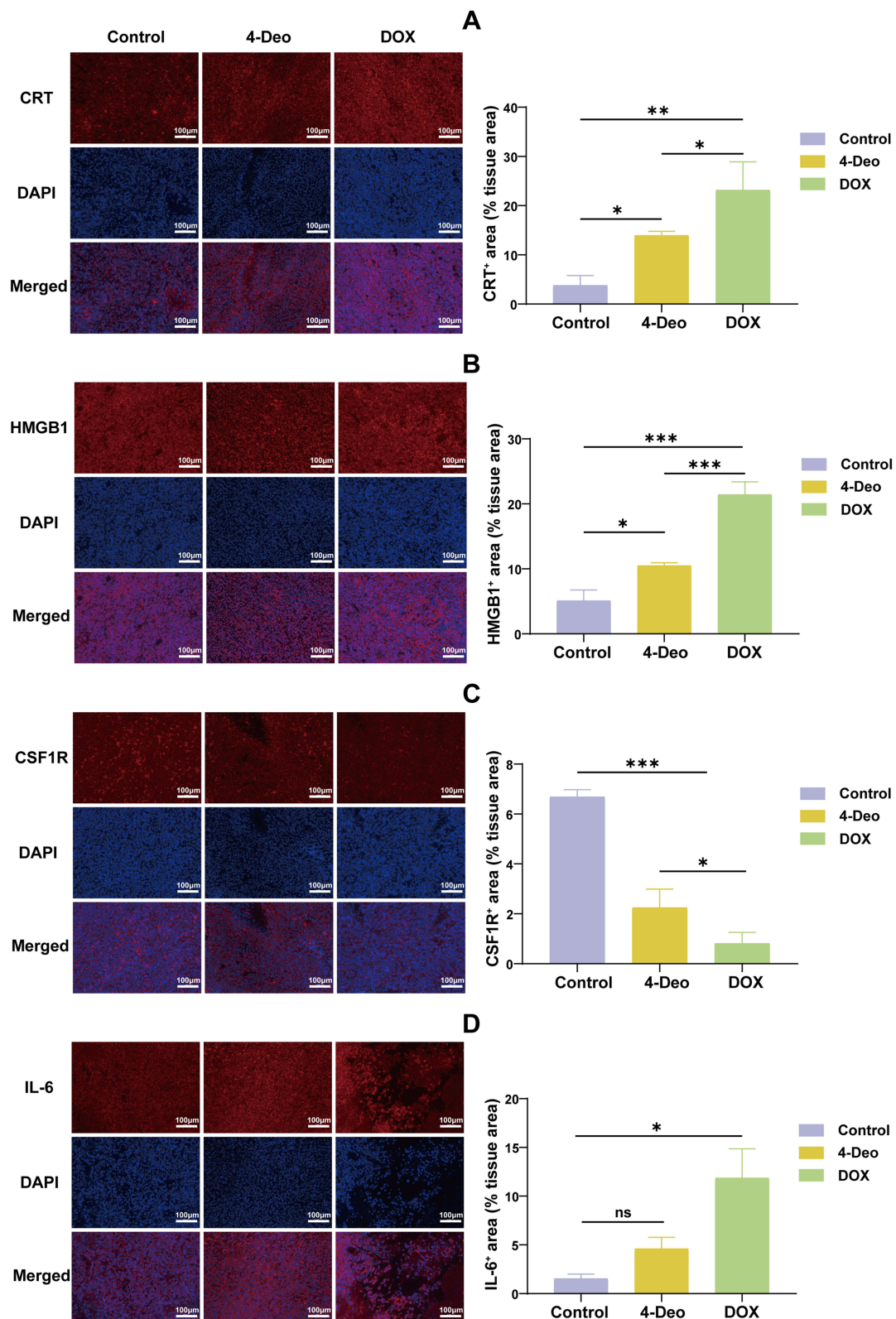


Figure 5 Immunohistochemical examination of 4-Deo. Labeling with different antibodies at the end of the experiment to detect immunohistochemistry of tumor tissue. (A) CRT, (B) HMGB1, (C) CSF1R, (D) IL-6. All data are presented as mean \pm SD (n = 5). ns p > 0.05, *p < 0.05, **p < 0.01, ***p < 0.001.

DOX group and the 20% in the control group (Figure 4B). Figure 4D was a picture of a solid tumor at the end of the experiment. Compared to the initial body weight, at the endpoint of the experiment, there was an increase in body weight in the control, DOX and 4-Deo groups. This was due to the fact that as the tumor grew, its weight occupied an increasing proportion of the mice's body weight. However, the mice in the 4-Deo group did not show significant changes in body weight, which indicated that it had a good inhibitory effect on hepatocellular carcinoma, which was corroborated with the data on tumor volume (Figure 4C). As we all know, multidrug resistance and severe cardiac toxicity are important limitations of anthracycline drug therapy.^{34,35} Fortunately, HE results showed that 4-Deo could alleviate the cardiotoxicity of DOX to a certain extent, and there was no significant difference between the groups for other organs, indicating that it did not produce significant damage to the mice and that the safety of 4-Deo is acceptable (Figure 4E). 4-Deo has a similar therapeutic effect with DOX but does not cause serious damage to important organs, which is a unique advantage of 4-Deo different from DOX. In summary, 4-Deo is similar to DOX in terms of tumor-suppressing effects, and it has an acceptable safety that will not limit its use, so the promise of 4-Deo research is surprising.

4-Deo Induced Immune Response

After animal experiments demonstrated that 4-Deo was a significant tumor suppressor, preliminary explorations of how 4-Deo exerted its pharmacological effects in vivo were developed. After treatment of tumor tissue sections with different antibodies, it was found that 4-Deo exhibited potential in inhibiting tumor growth by triggering immunogenic cell death (ICD) and regulating tumor-associated macrophages (TAMs) polarization.

Immunogenic cell death (ICD) is a form of cancer cell death that can be triggered by certain chemotherapy drugs.³⁶ The main feature of ICD is the release of damage-associated molecular patterns (DAMPs) from dying tumor cells, such as calreticulin (CRT), adenosine triphosphate (ATP) and high mobility group box 1 (HMGB1).^{37–39} These DAMPs can directly bind to and activate dendritic cells (DCs), thereby attracting T cells into tumor microenvironment (TME).⁴⁰ Anthracyclines are the representative drugs of ICD, they can not only induce cancer cell death but also stimulate anti-tumor immunity by inducing ICD.^{41,42} However, since DOX-induced ICD is too weak and tumor recurrence is often observed, it is necessary to develop new anticancer drugs or lead compounds.⁴⁰ Since 4-Deo has a similar parent structure to DOX, CRT and HMGB1 antibodies were used to test whether 4-Deo has the potential to induce ICD. Antibody labeling of CRT and HMGB1 showed that 4-Deo was able to induce ICD, but its induction was lower than that of DOX (Figure 5A and B). Thus, 4-Deo may also play a role in tumor inhibition through other pathways.

Unique TME exists in hepatocellular carcinoma, and TAMs are major components of the TME.^{43,44} TAMs may exhibit two activation phenotypes: a classically activated state (M1) and an alternatively activated state (M2).⁴⁵ TAMs of the M1 phenotype promote inflammation and are thought to have antitumor activity, whereas TAMs of the M2 phenotype have anti-inflammatory and tumor growth-promoting effects.^{46,47} Therefore it is speculated that 4-Deo may modulate the phenotypes of TAMs thereby achieving tumor suppression. CD86 is a marker of M1,^{48,49} so the sections were labeled with CD86 antibody. It can be seen that the mice in the 4-Deo group had a strong signal of CD86 at the tumor site, and the positive area was significantly more than the control and DOX (Supplementary Figure S2). Interleukin 6 (IL-6) is a pro-inflammatory factor secreted by M1.⁵⁰ Figure 5D shown that compared with the control group, IL-6 in the 4-Deo group increased but there was no significant difference. Therefore, we speculate that 4-Deo may have the ability to induce TAMs to M1. Stimulation of Colony Stimulating Factor-1 (CSF-1) causes TAMs often tend to be polarized to an M2-like state, which in turn promotes angiogenesis and massive secretion of tumorigenic cytokines to promote tumor growth.^{51,52} Therefore, using antibodies to label Colony-Stimulating Factor-1 Receptor (CSF1R), the results showed that the CSF1R in the 4-Deo group was less obvious than that in the control group (Figure 5C), which could significantly reduce the expression of CSF-1, block the transformation of TAMs to M2 phenotype, and then play a role in suppressing tumors. Compared with M1 phenotype, M2 usually accounts for a larger proportion of TME in solid tumors and leads to tumor immune escape,⁵³ so inhibiting the conversion of TAMs to the M2 phenotype is helpful for tumor suppression.

Conclusions

4-Deo, isolated from the fermentation product of *Streptomyces* sp. BG-11, has a certain anti-tumor ability. It is worth our attention that the safety of 4-Deo was far superior to DOX and has the potential to be a promising anti-cancer drug or

lead compound. In vitro experiments have proved that 4-Deo can inhibit the proliferation of tumor cells by inducing cell necrosis and blocking cells in S phase. In vivo assays showed that 4-Deo exhibited great potential in inhibiting tumor growth by triggering immunogenic cell death (ICD) and regulating tumor-associated macrophages (TAMs) polarization. In summary, this paper demonstrated the promise of 4-Deo as a drug or lead compound for cancer treatment, filling the current gap in the research on the pharmacological effects of 4-Deo.

Acknowledgments

We appreciate the great experimental support from the Public Platform of Pharmaceutical Research Center, Academy of Chinese Medical Science, Zhejiang Chinese Medical University. This study was supported by the Zhejiang Provincial Natural Science Foundation of China (LY23H280010) and the Research Project of Zhejiang Chinese Medical University (2023JKZKTS23). Graphical abstract created with BioRender.com.

Disclosure

The authors declare no conflicts of interest in this work.

References

1. Bray F, Laversanne M, Sung H, et al. Global cancer statistics 2022: GLOBOCAN estimates of incidence and mortality worldwide for 36 cancers in 185 countries. *Ca a Cancer J Clinicians*. 2024. doi:10.3322/caac.21834
2. Mohamed K, Rzymiski P, Islam MS, et al. COVID-19 vaccinations: the unknowns, challenges, and hopes. *J med virol*. 2022;94(4):1336–1349. doi:10.1002/jmv.27487
3. Malik JA, Mulla AH, Farooqi T, Potttoo FH, Anwar S, Rengasamy KRR. Targets and strategies for vaccine development against SARS-CoV-2. *Biomed Pharmacoth*. 2021;137:111254. doi:10.1016/j.biopha.2021.111254
4. Xue X, Lindstrom A, Qu H, Li Y. Recent advances on small-molecule nanomedicines for cancer treatment. *Wiley Interdisciplinary Rev Nanomed Nanobiotechnol*. 2020;12(3):e1607. doi:10.1002/wnan.1607
5. Zhao PJ, Wang HX, Li GH, Li HD, Liu J, Shen YM. Secondary metabolites from endophytic *Streptomyces* sp. Lz531. *Chem. Biodivers*. 2007;4(5):899–904. doi:10.1002/cbdv.200790078
6. Sang XN, Chen SF, Chen G, et al. Two pairs of enantiomeric α -pyrone dimers from the endophytic fungus *Phoma* sp YN02-P-3. *RSC Adv*. 2017;7(4):1943–1946. doi:10.1039/c6ra26319d
7. Zhu Y, Zhang W, Chen J. Binary Nanodrug-Delivery System Designed for Leukemia Therapy: aptamer- and Transferrin-Codecorated Daunorubicin- and Luteolin-Coloaded Nanoparticles. *Drug Des Devel Ther*. 2023;17:1–13. doi:10.2147/dddt.S387246
8. Zhao J, Lin E, Cai C, et al. Combined Treatment of Tanshinone I and Epirubicin Revealed Enhanced Inhibition of Hepatocellular Carcinoma by Targeting PI3K/AKT/HIF-1 α . *Drug Des Devel Ther*. 2022;16:3197–3213. doi:10.2147/dddt.S360691
9. Habibullah MM, Mohan S, Syed NK, et al. Human Growth Hormone Fragment 176-191 Peptide Enhances the Toxicity of Doxorubicin-Loaded Chitosan Nanoparticles Against MCF-7 Breast Cancer Cells. *Drug Des Devel Ther*. 2022;16:1963–1974. doi:10.2147/dddt.S367586
10. Zhang S, Wu P, Liu J, Du Y, Yang Z. Roflumilast Attenuates Doxorubicin-Induced Cardiotoxicity by Targeting Inflammation and Cellular Senescence in Cardiomyocytes Mediated by SIRT1. *Drug Des Devel Ther*. 2021;15:87–97. doi:10.2147/dddt.S269029
11. Liu J, Lane S, Lall R, et al. Circulating hemopexin modulates anthracycline cardiac toxicity in patients and in mice. *Sci Adv*. 2022;8(51):eadc9245. doi:10.1126/sciadv.adc9245
12. Bosman M, Krüger D, Van Assche C, et al. Doxorubicin-induced cardiovascular toxicity: a longitudinal evaluation of functional and molecular markers. *Cardiovascular Res*. 2023;119(15):2579–2590. doi:10.1093/cvr/cvad136
13. Ma A, Jiang K, Chen B, et al. Evaluation of the anticarcinogenic potential of the endophyte, *Streptomyces* sp. LRE541 isolated from *Lilium davidii* var. *unicolor* (Hoog) Cotton. *Microb Cell Fact*. 2021;20(1):217. doi:10.1186/s12934-021-01706-z
14. Yang X, Shang P, Yu B, et al. Combination therapy with miR34a and doxorubicin synergistically inhibits Dox-resistant breast cancer progression via down-regulation of Snail through suppressing Notch/NF- κ B and RAS/RAF/MEK/ERK signaling pathway. *Acta pharmaceutica Sinica B*. 2021;11(9):2819–2834. doi:10.1016/j.apsb.2021.06.003
15. Wei J, Chen X, Li Y, et al. Cucurbitacin B-induced G2/M cell cycle arrest of conjunctival melanoma cells mediated by GRP78-FOXM1-KIF20A pathway. *Acta pharmaceutica Sinica B*. 2022;12(10):3861–3876. doi:10.1016/j.apsb.2022.05.021
16. Kuerban K, Gao X, Zhang H, et al. Doxorubicin-loaded bacterial outer-membrane vesicles exert enhanced anti-tumor efficacy in non-small-cell lung cancer. *Acta Pharmaceutica Sinica B*. 2020;10(8):1534–1548. doi:10.1016/j.apsb.2020.02.002
17. Chen S, Dong G, Wu S, Liu N, Zhang W, Sheng C. Novel fluorescent probes of 10-hydroxyevodiamine: autophagy and apoptosis-inducing anticancer mechanisms. *Acta pharmaceutica Sinica B*. 2019;9(1):144–156. doi:10.1016/j.apsb.2018.08.003
18. Wei T, Xiaojun X, Peilong C. Magnoflorine improves sensitivity to doxorubicin (DOX) of breast cancer cells via inducing apoptosis and autophagy through AKT/mTOR and p38 signaling pathways. *Biomed Pharmacoth*. 2020;121:109139. doi:10.1016/j.biopha.2019.109139
19. Kciuk M, Gielecińska A, Mujwar S, et al. Doxorubicin-An Agent with Multiple Mechanisms of Anticancer Activity. *Cells*. 2023;12(4):659. doi:10.3390/cells12040659
20. Wang X, Hua P, He C, Chen M. Non-apoptotic cell death-based cancer therapy: molecular mechanism, pharmacological modulators, and nanomedicine. *Acta pharmaceutica Sinica B*. 2022;12(9):3567–3593. doi:10.1016/j.apsb.2022.03.020
21. Chen J, Kos R, Garssen J, Redegeld F. Molecular Insights into the Mechanism of Necroptosis: the Necrosome As a Potential Therapeutic Target. *Cells*. 2019;8(12):1486. doi:10.3390/cells8121486

22. Lopez A, Reyna DE, Gitego N, et al. Co-targeting of BAX and BCL-XL proteins broadly overcomes resistance to apoptosis in cancer. *Nat Commun.* 2022;13(1):1199. doi:10.1038/s41467-022-28741-7
23. Chaudhry GE, Md Akim A, Sung YY, Sifizul TMT. Cancer and apoptosis: the apoptotic activity of plant and marine natural products and their potential as targeted cancer therapeutics. *Front Pharmacol.* 2022;13:842376. doi:10.3389/fphar.2022.842376
24. Morana O, Wood W, Gregory CD. The Apoptosis Paradox in Cancer. *Int J Mol Sci.* 2022;23(3):1328. doi:10.3390/ijms23031328
25. He GW, Günther C, Thonn V, et al. Regression of apoptosis-resistant colorectal tumors by induction of necroptosis in mice. *J Exp Med.* 2017;214(6):1655–1662. doi:10.1084/jem.20160442
26. Hannes S, Karlowitz R, van Wijk SJL. The Smac mimetic BV6 cooperates with STING to induce necroptosis in apoptosis-resistant pancreatic carcinoma cells. *Cell Death Dis.* 2021;12(9):816. doi:10.1038/s41419-021-04014-x
27. Meier P, Legrand AJ, Adam D, Silke J. Immunogenic cell death in cancer: targeting necroptosis to induce antitumour immunity. *Nat Rev Cancer.* 2024;24(5):299–315. doi:10.1038/s41568-024-00674-x
28. Sun Y, Liu Y, Ma X, Hu H. The Influence of Cell Cycle Regulation on Chemotherapy. *Int J Mol Sci.* 2021;22(13):6923. doi:10.3390/ijms22136923
29. Hao G, Zhai J, Jiang H, et al. Acetylshikonin induces apoptosis of human leukemia cell line K562 by inducing S phase cell cycle arrest, modulating ROS accumulation, depleting Bcr-Abl and blocking NF- κ B signaling. *Biomed Pharmacother.* 2020;122:109677. doi:10.1016/j.biopha.2019.109677
30. Wang Y, Wu H, Dong N, et al. Sulforaphane induces S-phase arrest and apoptosis via p53-dependent manner in gastric cancer cells. *Sci Rep.* 2021;11(1):2504. doi:10.1038/s41598-021-81815-2
31. Navarro-Hortal MD, Varela-López A, Romero-Márquez JM, et al. Role of flavonoids against Adriamycin toxicity. *Food Chem Toxicol.* 2020;146:111820. doi:10.1016/j.fct.2020.111820
32. Aljobaily N, Viereckl MJ, Hydock DS, et al. Creatine Alleviates Doxorubicin-Induced Liver Damage by Inhibiting Liver Fibrosis, Inflammation, Oxidative Stress, and Cellular Senescence. *Nutrients.* 2020;13(1):41. doi:10.3390/nu13010041
33. Du W, Lu Q, Zhang M, Cao H, Zhang S. Synthesis and Characterization of Folate-Modified Cell Membrane Mimetic Copolymer Micelles for Effective Tumor Cell Internalization. *ACS Appl. Bio Mater.* 2021;4(4):3246–3255. doi:10.1021/acsabm.0c01612
34. Christidi E, Brunham LR. Regulated cell death pathways in doxorubicin-induced cardiotoxicity. *Cell Death Dis.* 2021;12(4):339. doi:10.1038/s41419-021-03614-x
35. Wu L, Wang L, Du Y, Zhang Y, Ren J. Mitochondrial quality control mechanisms as therapeutic targets in doxorubicin-induced cardiotoxicity. *Trends Pharmacol Sci.* 2023;44(1):34–49. doi:10.1016/j.tips.2022.10.003
36. Ahmed A, Tait SWG. Targeting immunogenic cell death in cancer. *Mol Oncol.* 2020;14(12):2994–3006. doi:10.1002/1878-0261.12851
37. Ma X, Yang S, Zhang T, et al. Bioresponsive immune-booster-based prodrug nanogel for cancer immunotherapy. *Acta Pharmaceutica Sinica B.* 2022;12(1):451–466. doi:10.1016/j.apsb.2021.05.016
38. Fucikova J, Kepp O, Kasikova L, et al. Detection of immunogenic cell death and its relevance for cancer therapy. *Cell Death Dis.* 2020;11(11):1013. doi:10.1038/s41419-020-03221-2
39. Zheng D, Liu J, Xie L, et al. Enzyme-instructed and mitochondria-targeting peptide self-assembly to efficiently induce immunogenic cell death. *Acta pharmaceutica Sinica B.* 2022;12(6):2740–2750. doi:10.1016/j.apsb.2021.07.005
40. Yu Z, Guo J, Hu M, Gao Y, Huang L. Icaritin Exacerbates Mitophagy and Synergizes with Doxorubicin to Induce Immunogenic Cell Death in Hepatocellular Carcinoma. *ACS nano.* 2020;14(4):4816–4828. doi:10.1021/acsnano.0c00708
41. Liang Q, Lan Y, Li Y, Cao Y, Li J, Liu Y. Crizotinib prodrug micelles co-delivered doxorubicin for synergistic immunogenic cell death induction on breast cancer chemo-immunotherapy. *Eur J Pharm Biopharmaceutics.* 2022;177:260–272. doi:10.1016/j.ejpb.2022.07.006
42. Kim M, Lee JS, Kim W, et al. Aptamer-conjugated nano-liposome for immunogenic chemotherapy with reversal of immunosuppression. *J Controlled Release.* 2022;348:893–910. doi:10.1016/j.jconrel.2022.06.039
43. Cheng K, Cai N, Zhu J, Yang X, Liang H, Zhang W. Tumor-associated macrophages in liver cancer: from mechanisms to therapy. *Cancer Commun.* 2022;42(11):1112–1140. doi:10.1002/cac2.12345
44. Xiang X, Wang J, Lu D, Xu X. Targeting tumor-associated macrophages to synergize tumor immunotherapy. *Signal Transduction Targeted Therapy.* 2021;6(1):75. doi:10.1038/s41392-021-00484-9
45. Cruceriu D, Baldasici O, Balacescu O, Berindan-Neagoe I. The dual role of tumor necrosis factor-alpha (TNF- α) in breast cancer: molecular insights and therapeutic approaches. *Cellular Oncology.* 2020;43(1):1–18. doi:10.1007/s13402-019-00489-1
46. Pan Y, Yu Y, Wang X, Zhang T. Tumor-Associated Macrophages in Tumor Immunity. *Front Immunol.* 2020;11:583084. doi:10.3389/fimmu.2020.583084
47. Munir MT, Kay MK, Kang MH, et al. Tumor-Associated Macrophages as Multifaceted Regulators of Breast Tumor Growth. *Int J Mol Sci.* 2021;22(12):6526. doi:10.3390/ijms22126526
48. Fang J, Ou Q, Wu B, et al. TcpC Inhibits M1 but Promotes M2 Macrophage Polarization via Regulation of the MAPK/NF- κ B and Akt/STAT6 Pathways in Urinary Tract Infection. *Cells.* 2022;11(17):2674. doi:10.3390/cells11172674
49. Luo G, Wang X, Cui Y, Cao Y, Zhao Z, Zhang J. Metabolic reprogramming mediates hippocampal microglial M1 polarization in response to surgical trauma causing perioperative neurocognitive disorders. *J Neuroinflammation.* 2021;18(1):267. doi:10.1186/s12974-021-02318-5
50. Arabpour M, Saghadzadeh A, Rezaei N. Anti-inflammatory and M2 macrophage polarization-promoting effect of mesenchymal stem cell-derived exosomes. *Int Immunopharmacol.* 2021;97:107823. doi:10.1016/j.intimp.2021.107823
51. Wen J, Wang S, Guo R, Liu D. CSF1R inhibitors are emerging immunotherapeutic drugs for cancer treatment. *Eur. J. Med. Chem.* 2023;245(Pt 1):114884. doi:10.1016/j.ejmech.2022.114884
52. Ramesh A, Brouillard A, Kumar S, Nandi D, Kulkarni A. Dual inhibition of CSF1R and MAPK pathways using supramolecular nanoparticles enhances macrophage immunotherapy. *Biomaterials.* 2020;227:119559. doi:10.1016/j.biomaterials.2019.119559
53. Wang S, Sun J, Dastgheyb RM, Li Z. Tumor-derived extracellular vesicles modulate innate immune responses to affect tumor progression. *Front Immunol.* 2022;13:1045624. doi:10.3389/fimmu.2022.1045624

Drug Design, Development and Therapy

Dovepress

Publish your work in this journal

Drug Design, Development and Therapy is an international, peer-reviewed open-access journal that spans the spectrum of drug design and development through to clinical applications. Clinical outcomes, patient safety, and programs for the development and effective, safe, and sustained use of medicines are a feature of the journal, which has also been accepted for indexing on PubMed Central. The manuscript management system is completely online and includes a very quick and fair peer-review system, which is all easy to use. Visit <http://www.dovepress.com/testimonials.php> to read real quotes from published authors.

Submit your manuscript here: <https://www.dovepress.com/drug-design-development-and-therapy-journal>